Proc. Natl. Acad. Sci. USA
Vol. 83, pp. 5469–5473, August 1986
Biochemistry

Hydroxyl radical "footprinting": High-resolution information about DNA–protein contacts and application to λ repressor and Cro protein

[iron(II) EDTA/Fenton reaction/DNA–protein interaction]

THOMAS D. TULLIUS AND BETH A. DOMBROSKI

Department of Chemistry, The Johns Hopkins University, Baltimore, MD 21218

Communicated by Donald D. Brown, April 18, 1986

ABSTRACT **A method has been developed for making "footprints" of proteins bound to DNA. The hydroxyl radical, generated by reduction of hydrogen peroxide by iron(II), is the reagent used to cut the DNA. Hydroxyl radical breaks the backbone of DNA with almost no sequence dependence, so all backbone positions may be monitored for contact with protein. In addition to defining the DNA sequence in contact with the protein, hydroxyl radical footprints embody structural information about the DNA–protein complex. For example, hydroxyl radical footprints of the bacteriophage λ repressor and Cro protein show directly that these proteins are bound to only one side of the DNA helix. Additional contacts of λ repressor and Cro protein with DNA, not observed by other chemical footprinting methods, are revealed by hydroxyl radical footprinting.**

The first question to be asked about any protein that makes a complex with DNA is, "To what DNA sequence does the protein bind?" Galas and Schmitz introduced the most widely used technique for answering this question, DNase I "footprinting" (1). Several variations on the original footprinting method, using reagents other than DNase I, have been developed since that time (2, 3). All of these methods work by using a reagent (enzymatic or chemical) that will cut the backbone of DNA. A protein will inhibit the cutting reaction at sites on the DNA to which it is bound, leaving a blank in the cutting pattern, which is aptly dubbed the "footprint" of the protein.

We have devised a footprinting technique that overcomes many of the limitations of previous methods and gives the most detailed footprints yet of proteins bound to DNA. We make use of a chemical reagent that cleaves the DNA backbone with virtually no dependence on base sequence. This reagent, hydroxyl radical (4), is conveniently generated by iron(II)-promoted reduction of dioxygen or hydrogen peroxide (5). Hydroxyl radical is thought to attack the deoxyribose sugars arrayed along the surface of DNA (6). Secondary reactions of the resulting deoxyribose-centered radicals eventually cause the backbone to break, in essence by disintegration of the sugars themselves (7).

We demonstrate here that hydroxyl radical can make footprints of the bacteriophage λ repressor and Cro proteins bound to the O_R1 operator sequence. We find that backbone deoxyriboses that are occluded by bound protein are cut with decreased efficiency by the radical. The result is a set of bands of reduced intensity in the sequencing gel pattern, which correspond to the points of contact of the protein with the DNA backbone. All backbone positions of the DNA molecule are observed, since the radical reacts with each deoxyribose with no sequence or base specificity (4, 6, 8). Since hydroxyl radical is so small (roughly the size of a water molecule) very tight footprints are seen, giving sharp definition of the protein–DNA contacts along the backbone. In fact, for λ repressor and Cro protein we are able to produce footprints that clearly show that these proteins are bound to only one side of the helix; the "backside" of the DNA molecule, not covered by protein, is still cut efficiently by hydroxyl radical. Our results agree well with λ repressor–DNA and Cro–DNA contacts inferred from methylation protection and interference, ethylation interference, and DNase I footprinting experiments (9, 10), and with the basic features of the proposed complexes (11), but provide additional information about the structures of these protein–DNA complexes.

EXPERIMENTAL PROCEDURES

Enzymes and Chemicals. The restriction endonucleases *Bgl* II and *Eco*RI were obtained from Bethesda Research Laboratories and were used as recommended by the manufacturer. Calf intestinal alkaline phosphatase and the Klenow fragment of DNA polymerase I came from Boehringer Mannheim, DNase I was from Worthington, and T4 polynucleotide kinase was from Pharmacia P-L Biochemicals. Ammonium iron(II) sulfate hexahydrate $[(NH_4)_2Fe(SO_4)_2 \cdot 6H_2O]$ and EDTA (disodium salt; Gold Label) were purchased from Aldrich, L-ascorbic acid (sodium salt) was from Sigma, and hydrogen peroxide (as a 30% solution) was from J. T. Baker Chemical (Phillipsburg, NJ). Radioactive nucleotides were obtained from Amersham. Water was purified through a Millipore Milli-Q system.

DNA Preparation. Plasmid pOR1 (10), and its 120-base-pair (bp) *Eco*RI-*Bgl* II fragment, which contains the O_R1 operator sequence, were generous gifts from M. Brenowitz and G. Ackers. We also prepared end-labeled 120-bp restriction fragment by digesting pOR1 with *Bgl* II, labeling the ends with radioactive phosphorus, digesting with *Eco*RI, and purifying the labeled 120-bp fragment by electrophoresis on a low melting temperature agarose gel. We labeled the 3′ end (12) farthest from the O_R1 sequence by allowing *Bgl* II-cut pOR1 to react with the Klenow fragment of DNA polymerase I along with [α-^{32}P]dGTP (for the experiment in Fig. 1), or with dGTP, dATP, [α-^{32}P]TTP, and dideoxy CTP (for the experiment in Fig. 3). Reaction of *Bgl* II-cut pOR1, first with calf intestinal alkaline phosphatase, and then with T4 polynucleotide kinase and [γ-^{32}P]ATP, served to label the 5′ end (12) farthest from the O_R1 sequence.

Repressors. λ repressor was generously provided by M. Brenowitz and G. Ackers. J. Berg and C. Pabo kindly gave us a sample of Cro protein (originally prepared by A. Pakula and R. Sauer). Purity of the proteins was assessed by

The publication costs of this article were defrayed in part by page charge payment. This article must therefore be hereby marked "*advertisement*" in accordance with 18 U.S.C. §1734 solely to indicate this fact.

Abbreviation: bp, base pair(s).

$NaDodSO_4$/polyacrylamide gel electrophoresis. One band was seen for each, at the correct molecular weight.

Hydroxyl Radical Footprinting. End-labeled DNA (2 μl) was added to a buffer (10) consisting of 10 mM Bis Tris·HCl/0.1 mM EDTA/50 mM KCl/1 mM $CaCl_2$/0.5 μg of carrier (nucleosomal) DNA/bovine serum albumin at 100 μg/ml, pH 7.0. The volume of the reaction mixture at this point was 147 μl. Repressor–operator complex was prepared by adding 20 μl of a solution of repressor at the appropriate concentration to the reaction mixture and incubating at 37°C. A stock solution of iron(II) EDTA was prepared immediately before use by mixing equal volumes of freshly prepared 0.4 mM Fe(II) (aqueous) [by dissolution of $(NH_4)_2Fe(SO_4)_2 \cdot 6H_2O$] and 0.8 mM EDTA (aqueous). The footprinting reaction was initiated by placing iron(II) EDTA solution (10 μl), 0.6% hydrogen peroxide (10 μl), and 20 mM sodium ascorbate (10 μl) on the inner wall of the 1.5-ml Eppendorf tube containing the repressor–DNA mixture, allowing the reagents to mix, and then adding the cutting reagent to the repressor–DNA solution. The reaction was allowed to run for 2 min, then quenched by adding 0.1 M thiourea (20 μl), 3 M sodium acetate (25 μl), ethanol (750 μl), and tRNA (15 μg). The DNA was precipitated at −78°C, isolated by centrifugation, and the pellet was dissolved in a buffer consisting of 10 mM Tris·HCl/0.1 mM EDTA, pH 8.0. The mixture was extracted with phenol and the aqueous layer was washed with ether. Sodium acetate was added to 0.2 M and ethanol was added to 75%. The DNA was precipitated at −78°C, isolated by centrifugation, washed with cold 70% ethanol, dried using a Speed-vac concentrator, and dissolved in formamide/dye mixture (12).

DNase I footprinting reactions (1, 9, 10) were accomplished by adding DNase I (0.02 unit) to the repressor–DNA mixture described above and allowing the reaction to proceed for 1 min. The reaction was stopped by addition of 8 M ammonium acetate (50 μl), ethanol (750 μl), and tRNA (15 μg), and worked up as detailed above.

Gel Electrophoresis. DNA samples were run on 6% polyacrylamide/50% urea denaturing electrophoresis gels (0.4 mm thick) (13) at 1500 V for 2–4 hr. Gels were dried onto filter paper and autoradiographed at −70°C using preflashed (14) Kodax XAR-5 film and a Dupont Cronex Lightning Plus intensifying screen. Autoradiographs were scanned with a Joyce–Loebl Chromoscan 3 densitometer, with an aperture width of 0.05 cm.

RESULTS AND DISCUSSION

DNA Cleavage Chemistry. We used the EDTA complex of iron(II) [$Fe(EDTA)^{2-}$] as a reagent for generating hydroxyl radical from hydrogen peroxide (5, 6, 8). This chemistry is known as the Fenton or Haber–Weiss reaction. A negatively charged complex of iron(II) was used so the metal complex would not associate electrostatically with the DNA molecule. We think it is an advantage to limit the interaction of the iron reagent with the DNA–protein complex, so that the conformation of the DNA molecule is not altered by binding of the metal species, and so that the ultimate probe of the complex (hydroxyl radical) is as small as possible. A reducing agent, sodium ascorbate (15), was present in the reaction mixture to reduce the iron(III) product of the Fenton reaction back to iron(II), making it possible to produce footprints with micromolar concentrations of iron. We have found that this chemistry is compatible with many other buffer, pH, and salt conditions. The only species commonly found in solutions of DNA–protein complexes that we have observed to interfere with hydroxyl radical footprinting is glycerol, an efficient scavenger of hydroxyl radical. Dilution of glycerol to <0.5% restores the ability of the reagent to cut DNA.

The DNA molecule used in these experiments was a 120-bp long restriction fragment from plasmid pOR1 (10), which contains one copy of the 17-bp O_R1 operator of the bacteriophage λ, one of three related operator sequences in the right promoter of this phage. Reaction of hydroxyl radical with the DNA restriction fragment free of protein gave the products shown in Fig. 1 (lanes 4, 8, 10, and 14). We observe nearly equal cutting at each deoxyribose along the chain. Since a cutting "signal" is seen at every position in the sequence, we can monitor the effect of bound protein on the accessibility to hydroxyl radical of any position along the DNA backbone.

Hydroxyl Radical Footprints. Binding λ repressor or Cro protein to the DNA before cutting with hydroxyl radical results in reduction of cutting at particular deoxyriboses in the sequence. The extent of inhibition of cutting depends on the amount of protein added (compare Fig. 1, lanes 5–7 and 11–13). The central lane in each titration (lane 6 or 12) results from digestion of the DNA–protein complex while the protein concentration is at the value for half saturation of the DNA binding site (as determined separately by filter binding experiments performed under the conditions of our footprinting experiments). The flanking lanes (5 and 7, 11 and 13) result from a 10-fold higher or lower concentration of protein. We see very similar titration behavior for λ repressor and Cro protein, even though the ranges of protein concentration spanned by the two titrations are very different, demonstrating directly the different affinities of each protein for O_R1 (9).

Structural Information from Hydroxyl Radical Footprints. The most striking feature of the hydroxyl radical footprints shown in Fig. 1 is the presence of two strongly protected

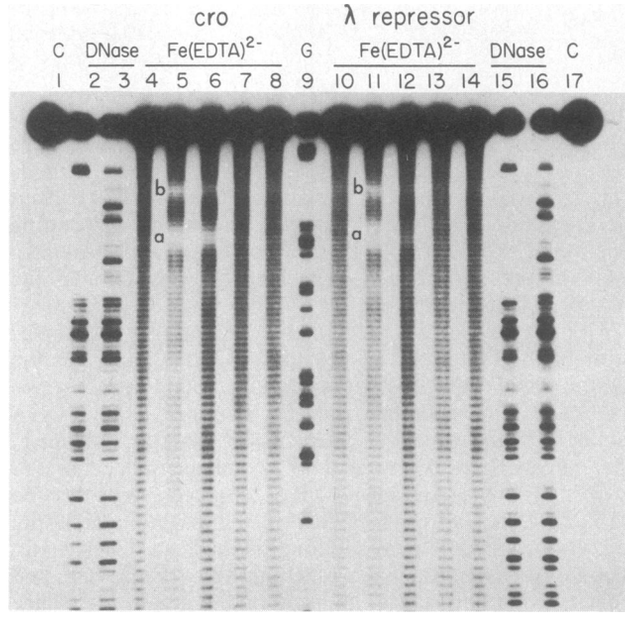

FIG. 1. Hydroxyl radical footprints of Cro protein and λ repressor bound to the O_R1 operator DNA sequence. Lanes 1 and 17, untreated 120-bp *Bgl* II/*Eco*RI restriction fragment, labeled at the 3′ *Bgl* II end. Lane 2, products of DNase I cutting of Cro protein–DNA complex (3.5 μM Cro). Lanes 3 and 16, products of DNase I cutting of the 120-bp restriction fragment, with no bound protein. Lanes 4, 8, 10, and 14, products of hydroxyl radical cutting of the 120-bp restriction fragment, with no bound protein. Lanes 5–7, products of hydroxyl radical cutting of Cro–DNA complex: lane 5, 3.5 μM Cro; lane 6, 350 nM Cro; lane 7, 35 nM Cro. Lane 9, products of the Maxam–Gilbert guanine-specific sequencing reaction (12). Lanes 11–13, products of hydroxyl radical cutting of λ repressor–DNA complex: lane 11, 90 nM λ repressor; lane 12, 9 nM λ repressor; lane 13, 900 pM λ repressor. Lane 15, products of DNase I cutting of λ repressor–DNA complex (90 nM repressor). Strong hydroxyl radical footprints are labeled a and b.

regions (labeled a and b) separated by a continuous set of unprotected backbone deoxyriboses. The centers of the two strongly protected regions are 10–11 bases apart. Cutting of four backbone positions between the protected sites is unaffected (or perhaps slightly enhanced) by bound protein.

The hydroxyl radical cutting patterns are consistent with the structures proposed for the complexes of λ repressor or Cro protein with DNA, which were based on computer graphics modeling starting from the x-ray crystal structures of the two proteins (11, 16–18). These models depict the proteins bound (as dimers) to only one side of the DNA molecule, with the backside of the DNA helix unencumbered by protein. Fig. 2*A* shows that the repressor–DNA contacts detected by hydroxyl radical lie on one side of a schematic of the B-DNA helix. The recent x-ray crystallographic study of the phage 434 repressor–DNA complex (19) shows that the same structure is adopted by this related protein–DNA complex.

Comparison with Other Footprinting Methods. Fig. 2*B* depicts the sequence of O_R1 and summarizes the results of chemical and enzymatic footprinting of λ repressor. The large featureless DNase I footprint (Fig. 1, lanes 2 and 15; Fig. 2*B*) gives no hint that λ repressor is bound to only one side of the DNA helix (11, 17, 18). DNase I cannot cut the exposed DNA backbone on the backside of the repressor–DNA complex, presumably because it cannot bind when there is a repressor protein bound to the other side of the DNA molecule. A DNase I footprint merely demarcates the DNA sequence that is bound by the protein.

In hydroxyl radical footprints, the minima and maxima of the cutting pattern are spanned by bands that vary smoothly in intensity, showing that some backbone positions are only partially blocked by bound protein from reaction with hydroxyl radical. We think the smooth variation in accessibility of the backbone to hydroxyl radical embodies details of the structure of the protein–DNA complex. The λ repressor–DNA and Cro–DNA complexes will be particularly attractive for evaluation of the structural information inherent in hydroxyl radical footprints, because co-crystals of both recently have been reported (20, 21).

Ethylation interference experiments have been used to define the contacts made by λ repressor with the phosphates along the DNA backbone (10). Since this technique reveals interactions of a protein with phosphates and not particular DNA bases, signals can be seen at every position along the chain. Fig. 2*B* shows that there is a close correspondence between phosphates important to λ repressor binding (10) and backbone deoxyriboses protected from reaction with hydroxyl radical by λ repressor. Ethylation interference defines four backbone regions (two on each strand of DNA) that interact with λ repressor (10), analogous to the four strong footprints (a, a′, b, and b′) produced by hydroxyl radical.

A difference, however, was noted between λ repressor and Cro protein in ethylation interference experiments (10). While λ repressor was found to interact with four sets of phosphates, Cro protein binding was reported to be affected only by ethylation of the two sets of phosphates near the dyad (corresponding to hydroxyl radical footprints a and a′). We were interested to see if hydroxyl radical footprints would show the same difference. We found, though, that the two repressors gave identical hydroxyl radical footprints (Fig. 1). A closer reading of the detailed report (10) of the ethylation interference experiments with Cro protein revealed a footnote stating that a few experiments showed that ethylation of another group of phosphates (corresponding to hydroxyl radical footprints b and b′) decreased Cro protein binding, but that these results were not consistent.

Ethylation interference experiments can be hard to reproduce, because the method requires the sometimes difficult separation of a DNA–protein complex from uncomplexed DNA. Interference with complexation can depend in subtle ways on salt concentration or other conditions (10), which also can lead to difficulties in reproducibility. Interference experiments identify which parts of the DNA cannot be alkylated without affecting complex formation (2, 22), while footprints show which parts of the DNA molecule are covered by protein. Hydroxyl radical footprinting, a much easier technique than interference methods, gives informa-

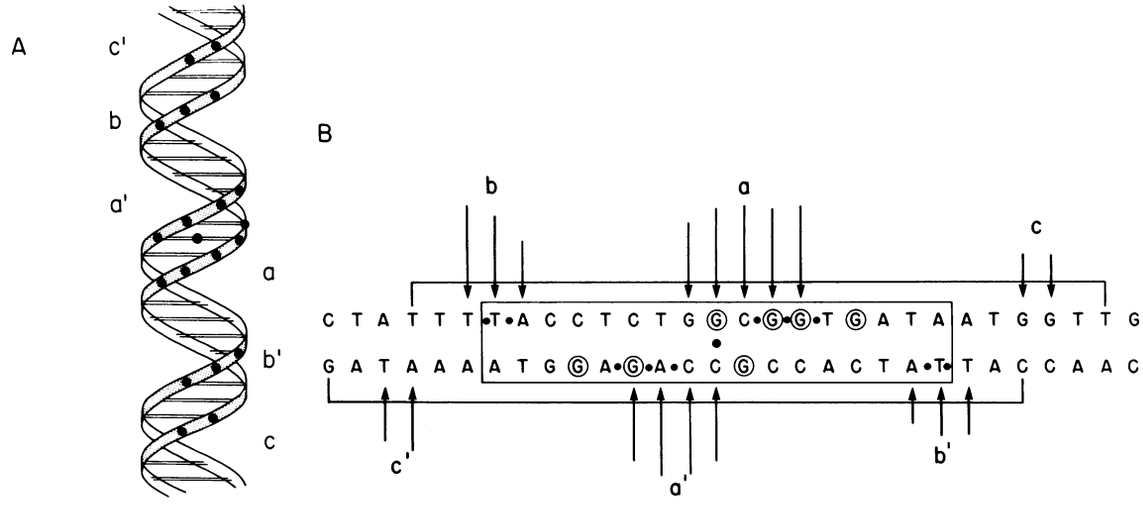

FIG. 2. Contacts of λ repressor with operator DNA. (*A*) Hydroxyl radical footprints mapped onto a scheme of B-DNA. Hydroxyl radical footprints are labeled a, b, c, a′, b′, and c′. The pseudo-dyad axis of the operator sequence is indicated by a filled circle in the center of the minor groove between footprints a and a′. Filled circles along the DNA backbone represent deoxyriboses protected by bound λ repressor from hydroxyl radical attack. These positions all occur on one side of the double helix. Footprints c and c′ are across the minor groove from footprints b and b′. (*B*) Summary of chemical and enzymatic footprinting of λ repressor bound to the O_R1 operator DNA sequence. The 17-bp O_R1 consensus sequence is boxed. The pseudo-dyad axis of the O_R1 sequence is indicated by a filled circle between the two sequences. Bases whose deoxyriboses are protected by bound λ repressor from attack by hydroxyl radical are indicated by vertical arrows; the length of the arrow is a rough measure of the protection afforded by repressor. DNase I footprints (10) are indicated by brackets above and below the sequence. Circled Gs represent guanines protected from methylation by bound λ repressor (10). Filled circles between letters represent phosphates whose ethylation interferes with binding of λ repressor (10).

tion on protein–backbone contacts that is complementary to results from ethylation interference experiments.

Methylation protection experiments (10) have shown that seven guanines, adjacent to the central pseudo-dyad axis of the O_R1 sequence, are protected by bound repressor from reaction with dimethyl sulfate (Fig. 2*B*). Almost all of these contacts are coincident with hydroxyl radical footprints a and a′. The two protein–DNA contact sites at the ends of the O_R1 sequence (revealed by hydroxyl radical footprints b and b′) consist solely of thymine [which does not react with dimethyl sulfate (2)] and adenine. [No effect of λ repressor or Cro protein on adenine methylation has been observed (10). This result implies that these proteins interact mainly with the major groove of DNA, since the position on adenine with which dimethyl sulfate reacts is in the minor groove.] Dimethyl sulfate is thus limited by its chemistry to revealing repressor–DNA contacts only near the center of the operator sequence.

Four of the seven guanines identified by methylation protection experiments as being occluded by λ repressor (10) are connected to deoxyriboses blocked from reaction with hydroxyl radical (Fig. 2*B*). Two other guanines that are protected by repressor from methylation, the farthest such guanines from the operator dyad (see Fig. 2*B*), are particularly interesting. A model of the proposed λ repressor–DNA complex (11, 17, 18) suggests that in these two regions λ repressor binds to the major groove but does not cover the DNA backbone, explaining why these two guanines do not react with dimethyl sulfate when repressor is bound, while their associated backbone deoxyriboses still can be cut by hydroxyl radical.

Repressor–DNA Interactions Beyond the Operator Sequence. Hydroxyl radical footprinting and ethylation interference experiments (10) agree that λ repressor makes contact with the DNA backbone on one side of the helix. These four backbone contact sites (two on each DNA strand) are located near the center and at the ends of the operator consensus sequence (Fig. 2*B*). Pairs of these sites (a and b′, a′ and b) define the edges of the major groove (Fig. 2*A*) within which the repressor is thought to make sequence-specific interactions with the DNA bases of the operator (11, 17, 18).

In addition to showing these four backbone contacts, hydroxyl radical footprinting also reveals protein–DNA interactions that extend beyond the 17-bp operator consensus sequence. These footprints are evident in Fig. 3, which shows hydroxyl radical footprints of λ repressor bound to O_R1, from the vantage points of both DNA strands. We produced these footprints with restriction fragments containing O_R1 labeled in two ways: either at the 3′ end (the top strand in Figs. 2*B* and 3), or at the 5′ end (the bottom strand) of the fragment farthest from the operator sequence.

Because of the approximate 2-fold symmetry of both the operator DNA sequence and the repressor dimer, hydroxyl radical footprints should be symmetrically disposed about the pseudo-dyad axis of the operator sequence. The autoradiograph in Fig. 3, and the densitometer scans in Fig. 4, clearly show this symmetry. The footprint nearest the dyad on the bottom strand (footprint a′) (Fig. 3, lanes 5 and 6) reflects across the dyad to give the corresponding footprint on the top strand (footprint a) (lanes 7 and 8). Similarly, the smaller strong footprint on the bottom strand (footprint b′) reflects across the dyad to give a corresponding footprint on the top strand (footprint b).

There also is a third set of footprints, c and c′, apparent in the experiment shown in Fig. 3. We find that footprints c and c′ also are produced by Cro protein (results not shown). While footprint c′ on the bottom strand is clearly visible in the autoradiograph (Fig. 3), footprint c, the symmetry-related footprint on the top strand, is most easily seen in the densitometer tracing (Fig. 4). These two footprints, not

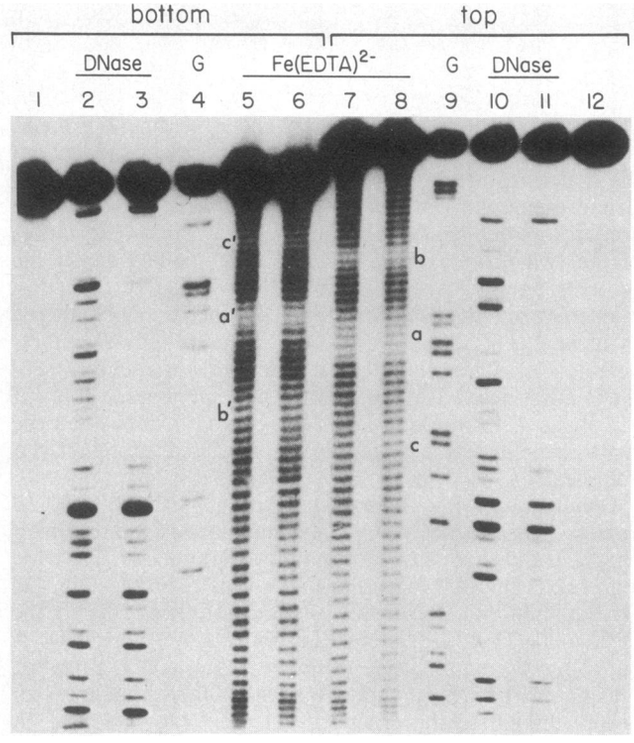

FIG. 3. Hydroxyl radical footprints of λ repressor on both strands of the 120-bp restriction fragment carrying the O_R1 operator sequence. "Bottom" and "top" refer to the DNA strands as drawn in Fig. 2*B*, and as diagrammed in Fig. 4. Labeling of the 5′ *Bgl* II end of the restriction fragment afforded data for the bottom strand, and labeling of the 3′ *Bgl* II end afforded data for the top strand. Lanes 1 and 12, untreated DNA, labeled on the bottom and top strands, respectively. Lanes 2 and 10, products of DNase I digestion of DNA labeled on the bottom and top strands, respectively, with no repressor present. Lanes 3 and 11, products of DNase I digestion of DNA labeled on the bottom and top strands, respectively, complexed with λ repressor (675 nM). Lanes 4 and 9, products of Maxam–Gilbert guanine-specific sequencing reactions (12) performed on DNA labeled on the bottom and top strands, respectively. Lanes 5 and 6, products of hydroxyl radical cutting of DNA labeled on the bottom strand, complexed with λ repressor. Lane 5, 90 nM λ repressor. Lane 6, 675 nM λ repressor. Lanes 7 and 8, products of hydroxyl radical cutting of DNA labeled on the top strand, complexed with λ repressor. Lane 7, 675 nM λ repressor. Lane 8, 90 nM λ repressor. The labels a, b, c, a′, b′, and c′ mark the hydroxyl radical footprints.

detected in ethylation interference experiments (10), extend to the ends of the DNase I footprints (Figs. 2*B* and 4). A model of B-DNA shows that footprints c and c′ are directly across the minor groove from the outer protein–DNA contacts detected by ethylation interference (10) (which correspond to hydroxyl radical footprints b′ and b; see Fig. 2).

The proposed structure of the λ repressor–DNA complex (11, 17, 18) does not incorporate contacts corresponding to footprints c and c′. This model uses straight B-form DNA and the λ repressor dimer, as found in the crystal structure of the protein, as elements of the proposed structure. Bending of the DNA [as suggested for the Cro–DNA and 434 repressor–DNA complexes (16, 19, 22)], or a change in the protein–protein contact in the repressor dimer (17), might permit interaction between protein and DNA at sites on the DNA backbone corresponding to footprints c and c′. Since the attenuation of backbone cleavage at footprints c and c′ is not as great as at footprints a and a′ (Fig. 4), footprints c and c′ could result from "shadowing" of the DNA backbone by the protein, and not from complete coverage.

The carboxyl end of helix 1 and the loop between helix 1 and helix 2 of the repressor (11) are the parts of the protein most likely to make these footprints. There are three lysines

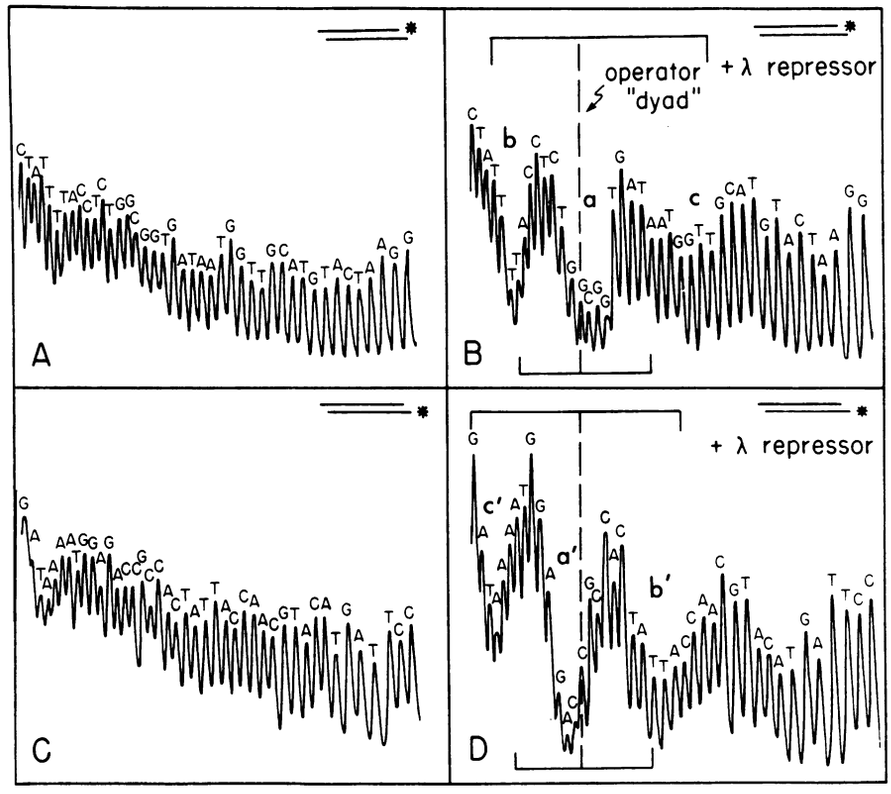

FIG. 4. Densitometer scans of hydroxyl radical footprints of λ repressor bound to the O_R1 operator DNA sequence. The letters above each peak represent the base whose attached deoxyribose was fragmented by reaction with hydroxyl radical. (*A* and *B*) DNA (120 bp) labeled at the 3′ *Bgl* II end (the top strand). (*C* and *D*) DNA (120 bp) labeled at the 5′ *Bgl* II end (the bottom strand). The schematic DNA molecule at the upper right corner of each panel shows the position of the radioactive label as an asterisk. (*A* and *C*) No repressor present. (*C* and *D*) λ repressor (675 nM) present (scans of lanes 7 and 6 in Fig. 3). In *B* and *D*, the horizontal bracket above each densitometer tracing represents the DNase I footprint of λ repressor on each strand, and the bracket below each tracing denotes the 17-bp operator consensus sequence. The broken vertical line passes through the pseudo-dyad axis of the O_R1 operator sequence. The labels a, b, c, a′, b′, and c′ mark the hydroxyl radical footprints.

(positions 24–26) near the possible contact site, which could be the amino acids that associate with the sugar–phosphate backbone and protect it from attack by hydroxyl radical (11). These backbone contacts probably do not mediate sequence-specific interactions of λ repressor with DNA, but more likely contribute to the free energy of binding. We anticipate that a high-resolution x-ray crystal structure of the complex (20) will show if our prediction is correct.

Concluding Remarks. We have shown that hydroxyl radical, produced by reduction of hydrogen peroxide by iron(II), is an ideal reagent for making footprints of proteins bound to specific sites on DNA. The simplicity of the reaction, combined with the innocuous character of the reagent (in contrast to traditional footprinting reagents such as dimethyl sulfate and ethylnitrosourea) also make this technique attractive. Especially when combined with results from other footprinting methods, such as DNase I footprinting, methylation protection and interference, and ethylation interference, hydroxyl radical footprints can provide detailed information on the structures of complexes of proteins with DNA.

We are grateful to Michael Brenowitz, Gary Ackers, Jeremy Berg, and Carl Pabo for providing us with DNA and repressor proteins, and for helpful discussions. This research was supported by grants from the Searle Scholars Program of the Chicago Community Trust, the National Institutes of Health (1 RO1 CA37444-01A1 and SO7 RR07041), and the Research Corporation.

1. Galas, D. J. & Schmitz, A. (1978) *Nucleic Acids Res.* **5,** 3157–3170.
2. Siebenlist, U. & Gilbert, W. (1980) *Proc. Natl. Acad. Sci. USA* **77,** 122–126.
3. Van Dyke, M. W. & Dervan, P. B. (1983) *Nucleic Acids Res.* **11,** 5555–5567.
4. Henner, W. D., Grunberg, S. M. & Haseltine, W. A. (1982) *J. Biol. Chem.* **257,** 11750–11754.
5. Bull, C., McClune, G. J. & Fee, J. A. (1983) *J. Am. Chem. Soc.* **105,** 5290–5300.
6. Hertzberg, R. P. & Dervan, P. B. (1984) *Biochemistry* **23,** 3934–3945.
7. Wu, J. C., Kozarich, J. & Stubbe, J. (1983) *J. Biol. Chem.* **258,** 4694–4697.
8. Tullius, T. D. & Dombroski, B. A. (1985) *Science* **230,** 679–681.
9. Johnson, A., Meyer, B. J. & Ptashne, M. (1979) *Proc. Natl. Acad. Sci. USA* **76,** 5061–5065.
10. Johnson, A. D. (1980) Dissertation (Harvard University, Boston, MA).
11. Pabo, C. O. & Sauer, R. T. (1984) *Annu. Rev. Biochem.* **53,** 293–321.
12. Maniatis, T., Fritsch, E. F. & Sambrook, J. (1982) *Molecular Cloning: A Laboratory Manual* (Cold Spring Harbor Laboratory, Cold Spring Harbor, NY).
13. Sanger, F. & Coulson, A. R. (1978) *FEBS Lett.* **87,** 107–110.
14. Laskey, R. & Mills, D. A. (1977) *FEBS Lett.* **82,** 314–316.
15. Udenfriend, S., Clark, C. T., Axelrod, J. & Brodie, B. B. (1954) *J. Biol. Chem.* **208,** 731–739.
16. Ohlendorf, D. H., Anderson, W. F., Fisher, R. G., Takeda, Y. & Matthews, B. W. (1982) *Nature (London)* **298,** 718–723.
17. Pabo, C. O. & Lewis, M. (1982) *Nature (London)* **298,** 443–447.
18. Lewis, M., Jeffrey, A., Wang, J., Ladner, R., Ptashne, M. & Pabo, C. O. (1983) *Cold Spring Harbor Symp. Quant. Biol.* **47,** 435–440.
19. Anderson, J. E., Ptashne, M. & Harrison, S. C. (1985) *Nature (London)* **316,** 596–601.
20. Jordan, S. R., Whitcombe, T. V., Berg, J. M. & Pabo, C. O. (1985) *Science* **230,** 1383–1385.
21. Brennan, R. G., Takeda, Y., Kim, J., Anderson, W. F. & Matthews, B. W. (1986) *J. Mol. Biol.* **188,** 115–118.
22. Bushman, F. D., Anderson, J. E., Harrison, S. C. & Ptashne, M. (1985) *Nature (London)* **316,** 651–653.